Biomedicine & Pharmacotherapy 155 (2022) 113729

Contents lists available at ScienceDirect

Biomedicine & Pharmacotherapy

journal homepage: www.elsevier.com/locate/biopha

ORIGINAL ARTICLE

The power of a novel combined anticancer therapy: challenge and opportunity of micotherapy in the treatment of Glioblastoma Multiforme

Ludovica Gaiaschi [a,1], Elisa Roda [a,b], Cristina Favaron [a], Federica Gola [a], Elisabetta Gabano [c], Mauro Ravera [c], Paola Rossi [d], Maria Grazia Bottone [a,*,2]

[a] Laboratory of Cell Biology and Neurobiology, Department of Biology and Biotechnology "L. Spallanzani", University of Pavia, Via Ferrata 9, 27100 Pavia, Italy
[b] Laboratory of Clinical and Experimental Toxicology, Pavia Poison Centre, National Toxicology Information Centre, Toxicology Unit, ICS Maugeri Spa, IRCCS, 27100 Pavia, Italy
[c] Department of Sciences and Technological Innovation (DiSIT), University of Piemonte Orientale "A. Avogadro", Viale Teresa Michel 11, 15121 Alessandria, Italy
[d] Laboratory of Neurophysiology and Integrated Physiology, Department of Biology and Biotechnology "L. Spallanzani", University of Pavia, Via Ferrata 9, 27100 Pavia, Italy

ARTICLE INFO

Keywords:
Glioblastoma Multiforme
Phytotherapy
Mitochondrial dysfunction
Oxidative stress
Ferroptosis
Drug resistance

ABSTRACT

Glioblastoma (GBM) is the most common and mortal primary brain tumor in human. After standard therapies, that include surgical resection followed by radiotherapy and chemotherapy, it is difficult to completely remove the tumor and the development of relapses and resistance is almost inevitable. The chemotherapy now available also show important side effects, to overcame those limitation, new platinum-based drugs are being synthetized, Pt(IV)Ac-POA, (OC-6–44)-acetate-diamine-chloride(2-(2-propynyl)octanoato)platinum(IV), a prodrug having an Histone-3-DeAcetylase-Inhibitor as axial ligands, is one of them. Moreover, new compounds of plant origin are increasingly seen as potential sources of benefits in oncological treatments. The aim of the study is to investigate the possible contribution of micotherapy in the fight against GBM, its role in the metabolism of reactive oxygen species (ROS) and its synergic effect with a new platinum-based compound, Pt(IV)Ac-POA, on human glioblastoma U251 cells. Through cytofluorimetric and immunofluorescence analysis, the ability of the micotherapy in study to regulate the cell cycle was assessed, and its importance in controlling the cellular redox state was also revealed, opening to the possibility of a new therapy in which micotherapy can support the activity of new chemotherapy while reducing its side effects controlling inflammatory conditions in the microenvironment. Additionally, the combined therapy appeared able to induce regulated form of necrosis, such as ferroptosis, and to hinder the establishment of resistance mechanisms.

1. Introduction

Glioblastoma (GBM) is the most common and lethal primary brain tumor in human, it had, indeed, an extremely poor prognosis with 5-year survival around 5 % [6,11]. GBM is a glioma, in particular a fourth-degree astrocytoma, a diffusive, invasive, vascularized and heterogeneous tumor, which grow into surrounding brain tissue. The US National Brain Tumor Society, in 2021, accounts that glioblastoma is the 14.3 % of all tumors and 49.1 % of all malignant tumors. IDH mutant glioblastomas account for approximately 10 % of all glioblastomas.

Currently, standard therapies include surgical resection followed by radiotherapy and chemotherapy; surgical operability depends on the anatomical location and extension of the tumoral mass [6]. The most widely used anti-tumor agent is radiotherapy and temozolomide (TMZ), a chemotherapy that acts as an alkylating agent to cause lethal DNA damage, but it leads to a median survival of 14.6 months. Despite of the initial response, development of resistance is almost inevitable, with 90 % of patients suffering from early disease recurrence [2].

The great intra- and inter-tumor heterogeneity defines the basis of therapeutic failure, thus, at the moment, there is no effective targeted

* Corresponding author.
E-mail addresses: ludovica.gaiaschi@unipv.it (L. Gaiaschi), elisa.roda@unipv.it (E. Roda), cristina.favaron01@universitadipavia.it (C. Favaron), federica.gola01@universitadipavia.it (F. Gola), elisabetta.gabano@uniupo.it (E. Gabano), mauro.ravera@uniupo.it (M. Ravera), paola.rossi@unipv.it (P. Rossi), mariagrazia.bottone@unipv.it (M.G. Bottone).
[1] ORCID: https://orcid.org/0000-0002-1880-2277.
[2] ORCID: https://orcid.org/0000-0003-4570-8785.

https://doi.org/10.1016/j.biopha.2022.113729
Received 20 July 2022; Received in revised form 13 September 2022; Accepted 19 September 2022
Available online 24 September 2022

therapy in the treatment of GBM.

Cisplatin (cis-dichlorodiammine platinum, CDDP), a metal-based alkylating agent, is the standard therapy for different types of solid tumors, including GBM. Cisplatin enters the cell via passive diffusion and DNA, with which it forms adducts, is the main target of its action. In particular cisplatin reacts preferentially with the N7 ring of adenine and guanine causing the establishment of cross-link DNA-protein and DNA-DNA. However, this molecule presents important side effects such as nephrotoxicity, neurotoxicity and ototoxicity. It also determines the onset of acquired drug resistance and consequently a reduction in its antitumor action [4,8].

In the endeavor to reduce systemic toxicity and enhance the anticancer activity a large number of molecules derived from platinum have been studied. Multi-action Pt(IV) drug have been synthesized, they are characterized by two axial ligands that, released along with the Pt(II) metabolite, can be synergistic or adjuvant agents.

Pt(IV)Ac-POA, (OC-6–44)-acetate diamine chloride (2-(2-propynyl) octanoato) platinum(IV), is a prodrug with two axial ligands, which are released together with the metabolite Pt (II) by reduction in the hypoxic microenvironment of cancer cells, limiting cytotoxicity in healthy tissues.

One of these ligands is an inert acetate, while the other is a medium chain fatty acid having Histone 3-DeAcetylase Inhibitor (HDACi) activity at the 9th lysine residue. Acetylation of histones allows access to the DNA also of the demethylases responsible for the removal of methyl groups; these modifications decrease DNA affinity for histones and increase de-condensation of chromatin.This appears to have a good effect on DNA adducts formation and chemo-sensitization [5].

Moreover, compounds of plant origin are increasingly recognized as potential sources in cancer therapy, as useful complementary treatments for oncological patients [12,27]. Those are considered valid alimentary sources of antioxidant substances that could interfere in the metabolism of reactive oxygen species (ROS) and defend the cells from damage caused by oxidative stress [24].

ROS are important bioproducts of cellular metabolism; mitochondria are a major source of ROS, suggesting their crucial role in maintaining cellular redox balance [11].

The balance between ROS production and scavenging is of high importance as ROS have been linked to numerous biological processes and disease conditions [7].

Most tumors show an increasing of ROS levels compared to normal tissues, an elevated ROS production would generate tumorigenesis by preventing DNA repair mechanisms, resulting in the accumulation of DNA damage, as well as an increase in cell proliferation [18]. Furthermore, oxidative stress controls it involved in the responsiveness of the tumor to treatments in multiple ways, including chemosensitivity, apoptosis, angiogenesis, metastasis and inflammatory responses [16].

Rising ROS levels have therefore been linked not only to the onset of cancer, but also to malignant transformation and resistance to chemotherapy [16,24].

However, the crucial role of ROS in various conditions is still controversial. On one hand an unregulated ROS formation is considered as a cause of pathological disease, on the other it is thought to be a downstream effect [24].

Another aspect that deserves to be evaluated is that if the increase in ROS reaches a certain threshold level which is incompatible with cell survival, ROS can exert a cytotoxic effect, leading to the death of malignant cells and thus limiting cancer progression. However, under conditions of persistent intrinsic oxidative stress, many cancer cells adapt well to it and develop antioxidant capacity [25]. Furthermore, GBM cells have a high metabolism and produce an extraordinary amount of ROS, accordingly, metabolic adaptation responsible for resistance in these cells deserves further studies [18]. Manipulating ROS levels in cancer cells could be an opportunity to selectively eliminate even highly drug-resistant tumor without causing significant off-target toxicity [25].

A crucial role in cell-wide stress responses has been given to OPA1 (optic atrophy-1), a member of the family of large GTPases. This protein is involved in the process of fusion of the inner mitochondrial membrane; loss of mitochondrial membrane potential in response to stress conditions may lead to disassembly of OPA1. This loss of fusion causes mitochondrial fission and deregulation of the mitochondrial structure and functionality. OPA1 homeostasis contributes to cell death pathways, proving a wider impact of mitochondrial dynamics on cellular survival [9].

Here, we evaluated the levels of protein involved in the response to oxidative stress condition. The superoxide dismutase 1, SOD1, constitutes the first line of defense against ROS generated by tissue and cellular damage. Similarly, SOD2, form of Mn-dependent superoxide dismutase, is found in the mitochondrial matrix where it catalyzes the free radical superoxide dismutase first into oxygen and then into H_2O_2. In cancer cells, overexpression of these enzymes is involved in the inhibition of the primary tumor and the proliferation of metastases, as ROS can produce mutations in DNA. The overexpression of SOD2 can also modulate the activity of nitric oxide by preventing its reaction with oxygen [2,7].

Mitochondrial cytochrome c oxidase (COX, complex IV) is the terminal electron acceptor of the mitochondrial respiratory chain that catalyzes the transfer of electrons from cytochrome c to molecular oxygen, contributing to the electrochemical gradient used by ATP synthase to form ATP [7]. COX4 is the last enzyme complex involved in the electron transport chain, so its alteration could potentially lead to the accumulation of ROS and oxidative stress. Its downregulation affects mitochondrial respiration, defining reduced oxygen consumption and ATP production, thus resulting in the induction of apoptosis in cells [1].

Among the features of oxidative stress in cells, lipid peroxidation in membrane bilayers has emerged as an important regulator of cell fate, leading cells to death via ferroptosis, a non-apoptotic cell death [13]. Iron is a key molecule for cell proliferation and function, but it can accumulate leading to cytotoxicity; ferroptosis can be initiated by iron-induced ROS production through the Fenton reaction, or by the activation of iron-containing enzymes such as lipoxygenases [28,29]. The aconitase 2 protein, ACO2, is an iron-containing enzymes characterized by a 4Fe-4S iron-sulfur cluster, that facilitates the elimination of the citrate hydroxyl group, the enzyme is, indeed, involved in the conversion of citric acid into isocitric acid in the tricarboxylic acid cycle [17], whose dysregulation is associated with tumor growth. In particular, the reduction of ACO2 would seem to be linked to mitochondrial dysfunction, with the release of Fe^{2+} and H_2O_2 ions as well as oxidative stress and ferroptosis [3].

The antiferroptosis activity of GSH, reduced glutathione, is mainly related to the protein glutathione peroxidase 4 (GPX4), which oxidizes GSH, acting as a phospholipid hydroperoxidase. GPX4 is also involved in antioxidant defense and the regulation of cell death [13].

Thanks to their antioxidant, anticancer, oncoimmunological and immunomodulating properties, compounds of fungal origin are gaining a new place in cancer therapy.

In this study we want to evaluate the effect of a mixture of mycelium and sporophores extracts of five species of medicinal mushrooms, including Agaricus blazei, Ophiocordyceps sinensis, Ganoderma lucidum, Grifola frondosa, and Lentinula edodes (Micotherapy U-care, A.V. D Reform s.r.l., Noceto, Parma, Italy) used in combination with traditional chemotherapy.

The properties of this phytotherapy have been previously described in the in vivo studies conducted by Roda et al. [21], in which the regulatory activity on cell proliferation, cell survival, cell invasion and angiogenesis, mainly determined by modulation of the immune response by fungal beta-glucans, emerged [21].

In the present study, we explored the effects induced by the combinate therapy of Micotherapy U-care with Cisplatin (cis-dichlorodiamine platinum (II)) and with a new prodrug, Pt(IV)Ac-POA, focusing on the link between oxidative stress and mitochondrial dysfunction, with the

purpose of finding a new strategy for anticancer therapy. The study is conducted on the human cell line U251, model for GBM and drug resistance properties.

2. Material and methods

2.1. Cell culture and treatment for U251 MG cell line

Human glioblastoma U251 MG cells were cultured in 75 cm^2 flasks in Eagle's minimal essential medium supplemented with 10 % fetal bovine serum, 2 % glutamine, 1 % sodium pyruvate, and 1 % of MEM non-essential amino acids solution and 100 U/ml penicillin and streptomycin in a 5 % CO_2 humidified atmosphere at 37 °C. 4 * 10^6 cells were plated in T75 flasks, or 6 * 10^5 cells were plated on coverslips positioned in 6-well plates, and treated, as below indicated, after 48 h having reached the 80 % of confluence. Then, cells were treated with CDDP 40 μM or Pt(IV)Ac-POA 10 μM for 48 h used alone or in combination with Micotherapy U-Care 5 mg/ml at continuous exposure. Chemotherapy concentrations were chosen by considering previous in vitro and in vivo experimental data [10,20], while micotherapy concentration was chosen according to the results obtained with the following experiment.

2.2. Flow cytometry

U251 cells were treated in 75 cm^2 flasks with Micotherapy U-Care for 48 h of continued exposure at 37 °C in a 5 % CO_2 humidified atmosphere. Three different concentrations were tested: 1 mg/ml, 5 mg/ml and 10 mg/ml. After treatments, cells were washed in sterile PBS, detached by trypsinisation and filtered with 40 μm cell strainers. The cells were washed in PBS, permeabilized in 70 % ethanol for 10 min, treated with RNase A 100 U/ml, and stained for 10 min at room temperature with propidium iodide 50 μg/ml (Sigma-Aldrich, Milan, Italy) 1 h. The preparation was processed with a Partec PAS III flow cytometer (Münster, Germany), PI red fluorescence was detected with a 610- nm long-pass emission filter. Data were analyzed with Flowing Software 2.5.1.

2.3. Immunofluorescence reactions

After treatment, cells grown on coverslips were fixed with 4 % formaldehyde for 20 min at room temperature and with 70 % ethanol for 24 h at − 20 °C. Samples were rehydrated in PBS-Tween 0.2 % and washed in PBS-Tween 0.2 %-BSA 4 % as blocking buffer, coverslips were then incubated in a humidified chamber with the primary antibodies (Table 1) prepared in PBS-Tween 0.2 % for 1 h at room temperature. After three washes, cells were incubated for 45 min with a solution of the secondary antibodies (Alexa 594 or 488 conjugated anti-mouse or anti-rabbit antibody, Alexa Fluor, Molecular Probes, Invitrogen) diluted at 1:200 in PBS-Tween 0.2 %. Nuclei were counterstained with 0.1 μg/ml of Hoechst 33,258 for 5 min, then washed twice in PBS 1X, and coverslips were mounted with Mowiol (Calbiochem).

2.4. Fluorescence microscopy and fluorescence intensity determination

An Olympus BX51 microscope was used. Images were recorded with an Olympus MagnaFire camera system and processed with the Olympus Cell F software. Each image related to the same marker in the experimental conditions was acquired with a constant exposure time selected on the control sample, making the fluorescence intensity comparable to avoid bias in the analysis. ImageJ Program was used to measure fluorescence intensity for quantitative analysis of protein expression.

The quantitative analysis of fluorescence intensity was carried out on 11 fields for each sample under analysis. In particular, the mean fluorescence intensity was calculated for each field of view net of background noise and, hence, the mean fluorescence intensity of the samples.

Table 1
Primary antibodies used for the fluorescence immunocytochemistry reactions.

Antigen	Primary antibody	Dilution in PBS
OPA1	Rabbit polyclonal anti-OPA1 (Abcam, Cambridge, UK)	1:200
SOD1	Rabbit polyclonal anti-SOD1 (Santa Cruz Biotechnology, Dallas, USA)	1:200
SOD2	Rabbit polyclonal anti-SOD2/MnSOD (Abcam, Cambridge, UK)	1:200
COX4	Mouse monoclonale [20E8C12] anti-COX4 (Abcam, Cambridge, UK)	1:200
ACO2	Rabbit polyclonal anti-Aconitase2 (Abcam, Cambridge, UK)	1:200
GPX4	Rabbit polyclonal anti-Glutathione Peroxidase 4 (Abcam, Cambridge, UK)	1:200
PCNA	Mouse monoclonale [PC10] anti-PCNA (Calbiochem, San Diego, USA)	1:200
H3K9ac	Rabbit polyclonal anti-Histone H3 (acetyl K9) (Abcam, Cambridge, UK)	1:100
CDC42	Rabbit polyclonal anti-CDC42 (Abcam, Cambridge, UK)	1:200
Mitochondria	Human autoimmune serum recognizing the 70 kDa E2 subunit of pyruvate dehydrogenase complex	1:200
Alpha-tubulin	Mouse monoclonal anti-Alpha-tubulin (Cell Signaling Technology, Danvers, USA)	1:1000
Beta-actin	Rabbit polyclonal anti-Beta-actin (GeneTex, Irvine, USA)	1:300

2.5. Statistical analyses

Analyses of mean value ± SEM were done using one-way ANOVA with Tukey test (GraphPad Prism 5.01). ρ values from $\rho < 0.05$ were considered statistically significant.

3. Results

3.1. Cell cycle cytofluorimetric assessment

In order to evaluate dose of usage and effect of Micotherapy U-Care on U251 cell line, the cells were exposed for 48 h to the mushrooms blend at concentrations of 10 mg/ml, 5 mg/ml and 1 mg/ml; subsequently they were fixed, colored with IP and analyze with flow cytometry. As shown in Fig. 1, at the dose 1 mg/ml there was an increase by 2.26 % of the number of cells in the G2/M phase. At 5 mg/ml there was a decrease by 6.99 % of cells in G1 and a increasing peak by 8.83 % corresponding to the G2/M phase, S-phase cells were reduced by 5.17 % compared to control condition. Furthermore, in this histogram, the presence of a new subpopulation, a sub-G1 peak (3.34 %) emerged. After treatment with Mic U-Care 10 mg/ml a further 6.36 % of the cells in G1 phase were observed, while the number of the population in the G2 phase was almost constant (8.63 %), the cells in the S phase returned increasing by 6.19 % compared to the sample treated with Mic U-Care 5 mg/ml, in addition, it has been possible to note the presence of a more defined sub-G1 peak (3.72 %).

The dose of micotherapy chosen for the subsequent studies has been 5 mg/ml, whose histogram featured a sub-G1 peak demonstrating the activation of cell death, moreover, the founding suggested that the use of this supplement could be useful for synchronizing cells in a single phase of the cell cycle and subsequently subjecting them to targeted chemotherapy treatment.

3.2. Immunocytochemical analysis of the redox equilibrium

Firstly, we conducted a doble-immunolabeling of OPA1 and mitochondria to evaluate their distribution and morphology (Fig. 2).

Mitochondria showed a homogenous distribution within the cytoplasm upon 48 h exposure to the treatments, nonetheless, their shape resulted more elongated after the treatment with the micotherapy 5 mg/

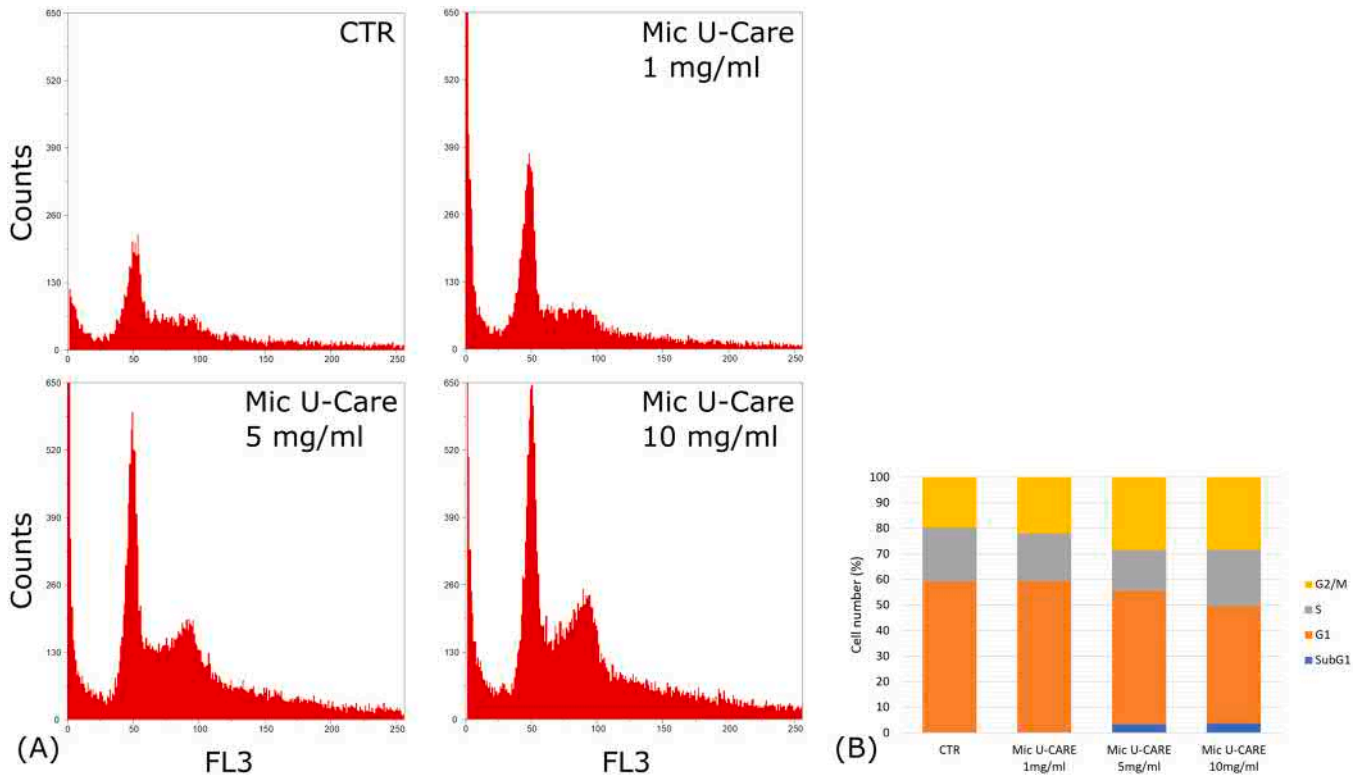

Fig. 1. U251 cells show different cell cycle features after the administration of different concentrations of Micotherapy U-Care. (A) Cytofluorimetric analysis of cell cycle status (Sub-G0, G0/G1, S, G2/M) of U251 cells, cytograms of the DNA content in U251 cells after IP staining, in control conditions (CTR) and after treatment with Micotherapy U-Care 1 mg/ml, 5 mg/ml and 10 mg/ml for 48 h. (B) Distributions of U251 cells in the cellular cycle phases after each treatment.

ml used alone. In combined therapy, with Cisplatin 40 μM + Mic U-Care 5 mg/ml and Pt(IV)Ac-POA 10 μM + Mic U-Care 5 mg/ml, the elongated mitochondria, a typical feature of drug resistance mechanism [22], were not visible, instead, it was observable an accumulation of these organelles in the nuclear periphery.

OPA1 labeling appeared diffuse and weak in the control, its intensity increased after the exposition to Mic U-Care 5 mg/ml. In this condition the colocalization of OPA1 and mitochondria was clear as like as in the cells treated with only Cisplatin 40 μM or Pt(IV)Ac-POA10 μM. After combined therapy with the mushroom mixture and chemotherapy, however, the colocalization hasn't been found so neat, in fact the staining appeared diffuser. OPA1, crucial protein to preserve normal mitochondrial crests, is more detectable, albeit in a non-statistically significant way, in samples treated with chemotherapeutic agents alone, in particular, after treatment with Cisplatin 40 μM. (Cisplatin + 39.85 %, SEM 0.53 ($\rho = 0.1558$), Cisplatin + Mic U-Care + 27.44 %, SEM 0.38, Pt(IV)Ac-POA + 35.05 %, SEM 0.64 ($\rho = 0.1951$), Pt(IV)Ac-POA + Mic U-Care + 22.41 %, SEM 0.34 (all vs. CTR)) (Table 2).

On the base of the results relating to mitochondrial functionality, we investigated the possible implication of therapy with Mic U-Care in the managing of cellular oxidative balance.

The first cellular line defense antioxidants include superoxide dismutase (SOD). Primarily, the distribution of SOD1 was evaluated through a doble-immunolabeling of this enzyme and alpha-tubulin (Fig. 3).

The tubulin cytoskeleton showed structure changes in the cells exposed to the micotherapy, it was possible to find morphological cell alteration, i.e. fusiform cell structure and more flattened nuclei. The treaties with CDDP 40 μM or Pt(IV)Ac-POA 10 μM revealed a collapsed cytoskeleton, modification in the cells organization were also observed after the combined treatments. In those cells, the nucleus is polylobed and segregated on the edges of the cell, moreover, in the same population coexist cells with collapsed cytoskeleton and others with a more orientated tubular structure.

The localization of SOD1 didn't change much from the control situation, it's homogeneous in the cytoplasm for all the cell samples, even if in the ones exposed to the micotherapy, fourth generation platinum therapy and the combination of the two the staining has been visible in the nuclear region, too. SOD1 is increased in samples receiving combination therapy and with micotherapy alone (+ 43.12 %, SEM 1.25 ($\rho = 0.0185$)). (Cisplatin + 12.43 %, SEM 0.55, Cisplatin + Mic U-Care + 40.57 %, SEM 1.21 ($\rho = 0.0317$), Pt(IV)Ac-POA + 20.98 %, SEM 0.55 and Pt(IV)Ac-POA + Mic U-Care + 42.46 %, SEM 1.38 ($\rho = 0.0213$) (all vs. CTR)) (Table 2).

Next, our attention moved on SOD2 and COX4, respectively shown in Figs. 4 and 5, as expected the was a clever localization of superoxide dismutase 2 and cytochrome c oxidase 4 in the mitochondria, that revealed the same features previously described, as the reduction in size after the micotherapy used together the chemotherapy. In the condition CDDP 40 μM + Mic U-Care 5 mg/ml and Pt(IV)Ac-POA 10 μM + Mic U-Care 5 mg/ml, the cells changed morphology with a decrease of the cell volume. Mitochondria lose their initial localization concentrating in the perinuclear area, probably as the result of a collapsed cytosolic organization. In this study, SOD2 expression increased in samples treated with combined therapies, particularly in Pt(IV)Ac-POA 10 μM + Mic U-Care 5 mg/ml treated samples. (Cisplatin + 3.72 %, SEM 0.61, Cisplatin + -Mic U-Care + 86.55 %, SEM 0.89 ($\rho < 0.0001$), Pt(IV)Ac-POA + 30.52 %, SEM 0.70 ($\rho = 0.0483$) and Pt(IV)Ac-POA + Mic U-Care + 109.35 %, SEM 1.15 ($\rho < 0.0001$) (all vs. CTR)) (Table 2) These finds could be significant of reduction of oxidative stress and therefore of a reduced tumorigenesis favored by the use of Mic U-Care.

In our samples, COX4 expression decreases in combined therapy, particularly with Cisplatin 40 μM + Mic U-Care 5 mg/ml, compared to respective chemotherapies used alone, (Cisplatin − 2.01 %, SEM 1.23, Cisplatin + Mic U-Care − 14.01 %, SEM 1.52, Pt(IV)Ac-POA + 31.30 %, SEM 1.55 and Pt(IV)Ac-POA + Mic U-Care + 26.60 %,

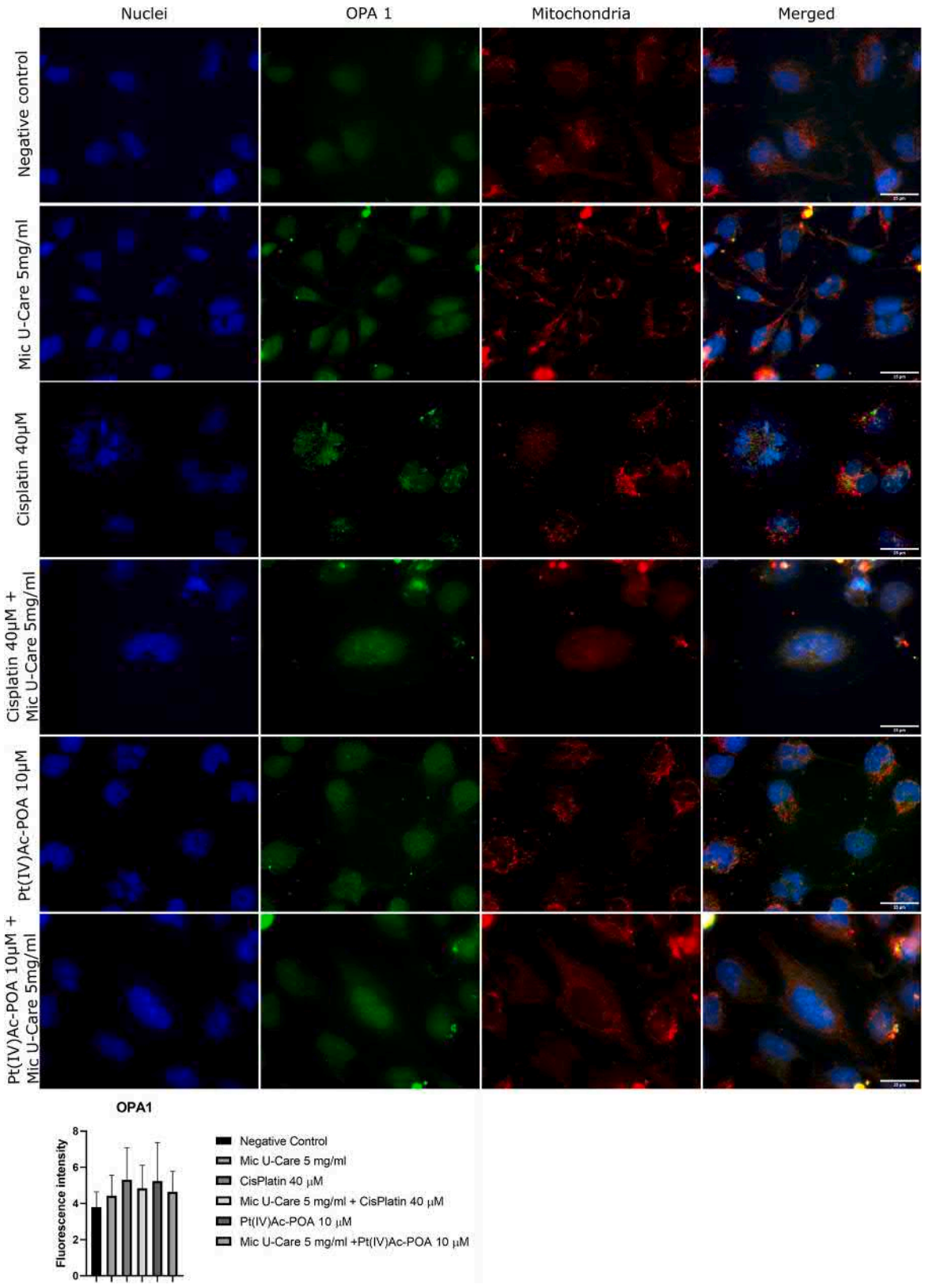

Fig. 2. Double immunolabeling for OPA1 protein (in green) and mitochondria (in red) in the controls, differently treated U251 cells, i.e., after 48 h-CT with Micotherapy U-Care 5 mg/ml, with CDDP 40 µM, with Pt(IV)Ac-POA 10 µM, with Mic U-Care + CDDP, with Mic U-Care + Pt(IV)Ac-POA. DNA was stained with Hoechst 33258 (blue fluorescence). Magnification 60X, bar of 25 µm. The histogram below shows the fluorescence intensity value of the immunolabeling. Statistical significance calculated as follows: *control vs. each experimental condition; #Mic U-Care vs. other treatments; §Cisplatin vs. Pt(IV)Ac-POA and each combined treatment; °Cisplatin + Mic U-Care vs. Pt(IV)Ac-POA and Pt(IV)Ac-POA + Mic U-Care; + Pt(IV)Ac-POA vs. Pt(IV)Ac-POA + Mic U-Care. ****$p < 0.0001$. ***$p < 0.001$; **$p < 0.01$; *$p < 0.1$.

Table 2
Summary of immunofluorescence results. Percentage fluorescence intensity (FI%) respect to the control condition with relative p Value.

	NC		Mic U-Care 5 mg/ml			CisPt 40 μM			Mic U-Care 5 mg/ml + CisPt 40 μM			Pt (IV)Ac-POA 10 μM			Mic U-Care 5 mg/ml + Pt (IV)Ac-POA 10 μM		
	FI %	SEM	FI %	SEM	p Value	FI %	SEM	p Value	FI %	SEM	p Value	FI %	SEM	p Value	FI %	SEM	p Value
OPA1	100.000	0.254	116.567	0.341	0.9099	139.850	0.537	0.1558	127.443	0.383	0.5451	138.048	0.642	0.1951	122.413	0.340	0.7396
SOD1	100.000	0.186	143.123	1.250	0.0185	112.430	0.551	0.93	140.566	1.208	0.0317	120.978	0.554	0.5933	142.458	1.383	0.0213
SOD2	100.000	0.127	119.251	0.824	0.4591	103.720	0.613	0.9992	186.545	0.885	< 0,0001	130.518	0.702	0.0483	209.353	1.147	< 0,0001
COX4	100.000	2.063	160.776	2.547	0.382	97.992	1.231	> 0,9999	85.988	1.518	0.9976	131.301	1.553	0.9145	126.595	1.735	0.9558
ACO2	100.000	0.224	135.711	0.323	< 0,0001	126.837	0.481	< 0,0001	64.294	0.281	< 0,0001	114.190	0.360	0.0772	96.822	0.356	0.9902
GPX4	100.000	0.248	139.452	1.225	0.0002	119.528	1.917	0.1599	89.210	0.788	0.775	127.612	1.737	0.0129	94.265	0.828	0.9813
PCNA	100.000	4.444	115.890	7.479	0.3435	40.809	3.212	< 0,0001	57.042	4.616	< 0,0001	71.264	5.107	0.0069	46.492	2.393	< 0,0001
H3K9ac	100.000	0.226	169.834	0.612	0.428	92.093	0.307	> 0,9999	230.701	2.201	0.0107	218.463	0.660	0.0271	250.998	1.154	0.002
Cdc42	100.000	0.445	93.127	0.503	0.9835	123.292	1.171	0.2089	86.845	0.404	0.7829	90.158	0.572	0.9246	82.605	0.455	0.5239

SEM 1.74 (all vs. CTR)) (Table 2), indicating a defect in mitochondrial function.

3.3. Immunocytochemical analysis of the ferroptotic pathway

To further investigate the oxidative stress pathway, the enzyme Aconitase 2 (Fig. 6) was considered. In the control samples the expression of ACO2 was diffuse in the cytoplasm, after the exposition to the chemotherapy the enzyme appears more concentrated in the perinuclear region where it partially colocalizes with the mitochondria. In the condition of combined therapy with CDDP 40 μM and Pt(IV)Ac-POA 10 μM + Micotherapy U-Care 5 mg/ml, a stronger colocalization of ACO2 and mitochondria is observed.

Aconitase 2 expression was lower in samples treated with combined therapy compared to chemotherapy alone, especially with micotherapy in combination with Cisplatin, this could be an indication of mitochondrial dysfunction and cause of a block of proliferation. (Cisplatin + 26.84 %, SEM 0.48 ($\rho < 0.0001$), Cisplatin + Mic U-Care- − 35.71 %, SEM 0.28 ($\rho < 0.0001$), Pt(IV)Ac-POA + 14.19 %, SEM 0.36 ($\rho = 0.0772$), Pt(IV)Ac-POA + Mic U-Care − 3.18 %, SEM 0.36 (all vs. CTR)) (Table 2).

Shrinkage of the mitochondria, as well as increase in their membrane density and reduction of mitochondrial crests, is a typical characteristic of ferroptosis. It has been evaluated the influence of the considered compounds on the activation of the ferroptosis pathway through the detection of glutathione peroxidase 4 (GPX4) (Fig. 7).

In the control cells, GPX4 is mainly localized in nucleoplasm and on the mitochondria; cells incubated with the different therapies exhibit the same distribution of GPX4 fluorescence. However, with the Pt(IV)Ac-POA and the mushrooms blend it seemed more homogeneously distributed outside the nucleus. GPX4 expression decreased in statistically significant way in samples receiving combination therapy in comparison with the counterpart chemotherapy. (Cisplatin + 19.53 %, SEM 1.92 ($\rho = 1599$), Cisplatin + Mic U-Care − 10.79 %, SEM 0.79, Pt (IV)Ac-POA + 27.61 %, SEM 1.74 ($\rho = 0.0129$) and Pt(IV)Ac-POA + -Mic U-Care − 5.74 %, SEM 0.83 (all vs. CTR)) (Table 2) This may be indicative of increased sensitivity to ferroptosis following combined therapy.

3.4. Immunocytochemical analysis of proliferation and migration

To study the role of the compounds considered in this study in the regulation of the proliferation and migration process, two specific markers such as PCNA and CDC42 were analyzed.

A double-immunolabeling of PCNA and H3K9ac was performed; as shown in Fig. 8, in all the samples PCNA localized in the nucleus, forming foci corresponding to the sites of ongoing DNA replication. In control conditions an intense signal was evident indicating the presence of active proliferating cells. After treatment whit chemotherapy and micotherapy, and in particular after the usage of Pt(IV)Ac-POA 10 μM alone and in combination with Mic U-Care 5 mg/ml, were noticeable whole cells without any staining. A labeling located out of the nucleus was also detectable suggesting a rupture of the nuclear membrane. Quantifying the fluorescence intensity of PCNA emerged an important reduction of the signal in the samples treated with chemotherapy, cells exposed to CDDP 40 μM shown a major decreasing compared to those exposed to Pt(IV)Ac-POA 10 μM, but the combined therapy of Pt(IV)Ac-POA 10 μM + Mic U-Care 5 mg/ml resulted equally effective. (Cisplatin − 59.19 %, SEM 3.21 ($\rho < 0.0001$), Cisplatin + Mic U-Care- − 42.96 %, SEM 4.62 ($\rho < 0.0001$), Pt(IV)Ac-POA − 28.74 %, SEM 5.11 ($\rho = 0.0069$) and Pt(IV)Ac-POA + Mic U-Care − 53.51 %, SEM 2.40 ($\rho < 0.0001$) (all vs. CTR)) (Table 2).

We evaluated the expression of H3K9ac, an epigenetic modification to the DNA packaging protein, to further characterized the action of the 2-propynyl-octanoic acid (POA) molecule as HDACi. As expected an important increase of H3K9ac was detectable in the samples treated

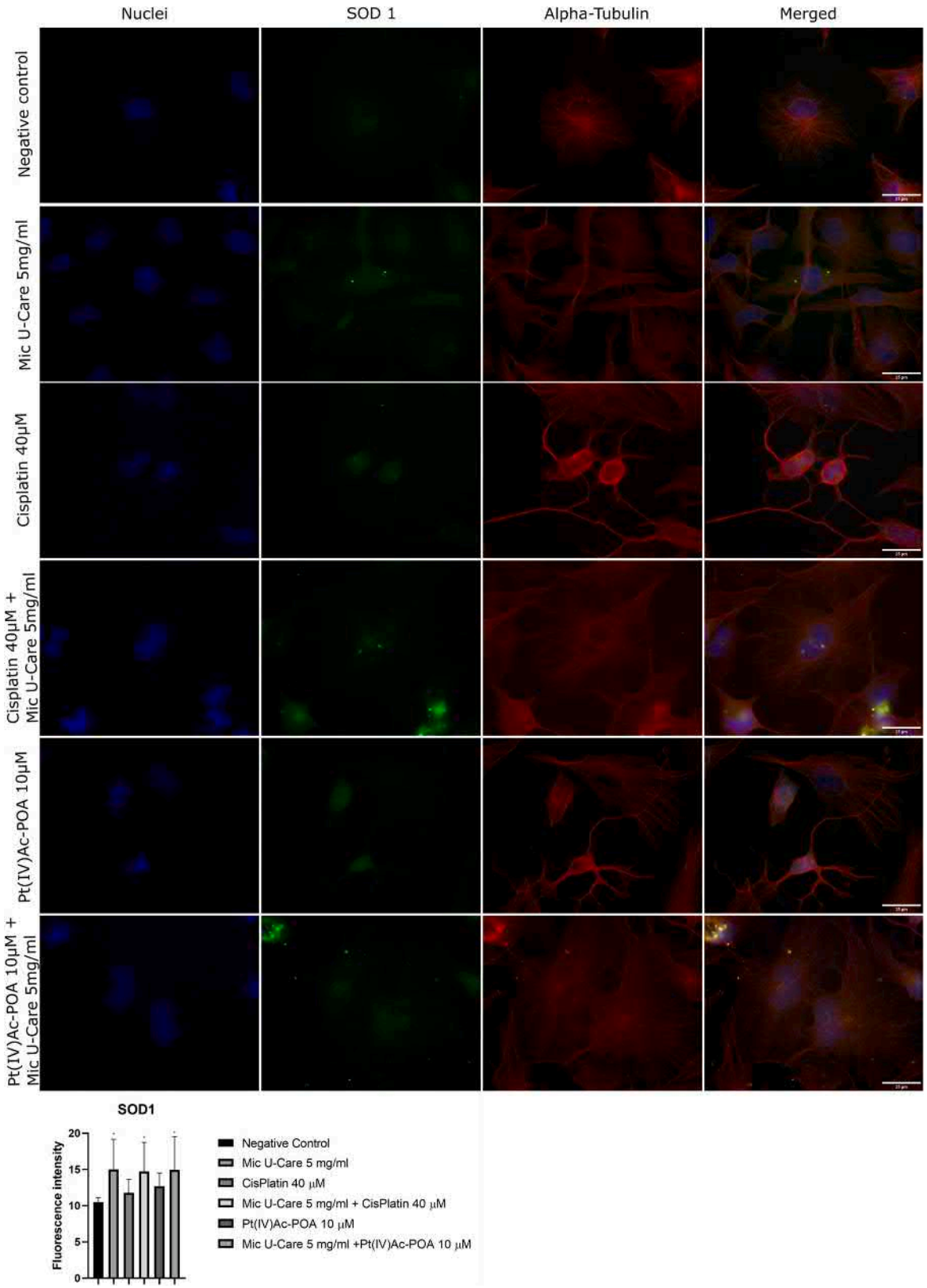

Fig. 3. Double immunolabeling for SOD1 protein (in green) and alpha-tubulin (in red) in the controls, differently treated U251 cells, i.e., after 48 h-CT with Micotherapy U-Care 5 mg/ml, with CDDP 40 µM, with Pt(IV)Ac-POA 10 µM, with Mic U-Care + CDDP, with Mic U-Care + Pt(IV)Ac- POA. DNA was stained with Hoechst 33258 (blue fluorescence). Magnification 60X, bar of 25 µm. The histogram below shows the fluorescence intensity value of the immunolabeling. Statistical significance calculated as follows: *control vs. each experimental condition; #Mic U-Care vs. other treatments; §Cisplatin vs. Pt(IV)Ac-POA and each combined treatment; °Cisplatin + Mic U-Care vs. Pt(IV)Ac-POA and Pt(IV)Ac-POA + Mic U-Care; + Pt(IV)Ac-POA vs. Pt(IV)Ac-POA + Mic U-Care. ****$p < 0.0001$. ***$p < 0.001$; **$p < 0.01$; *$p < 0.1$.

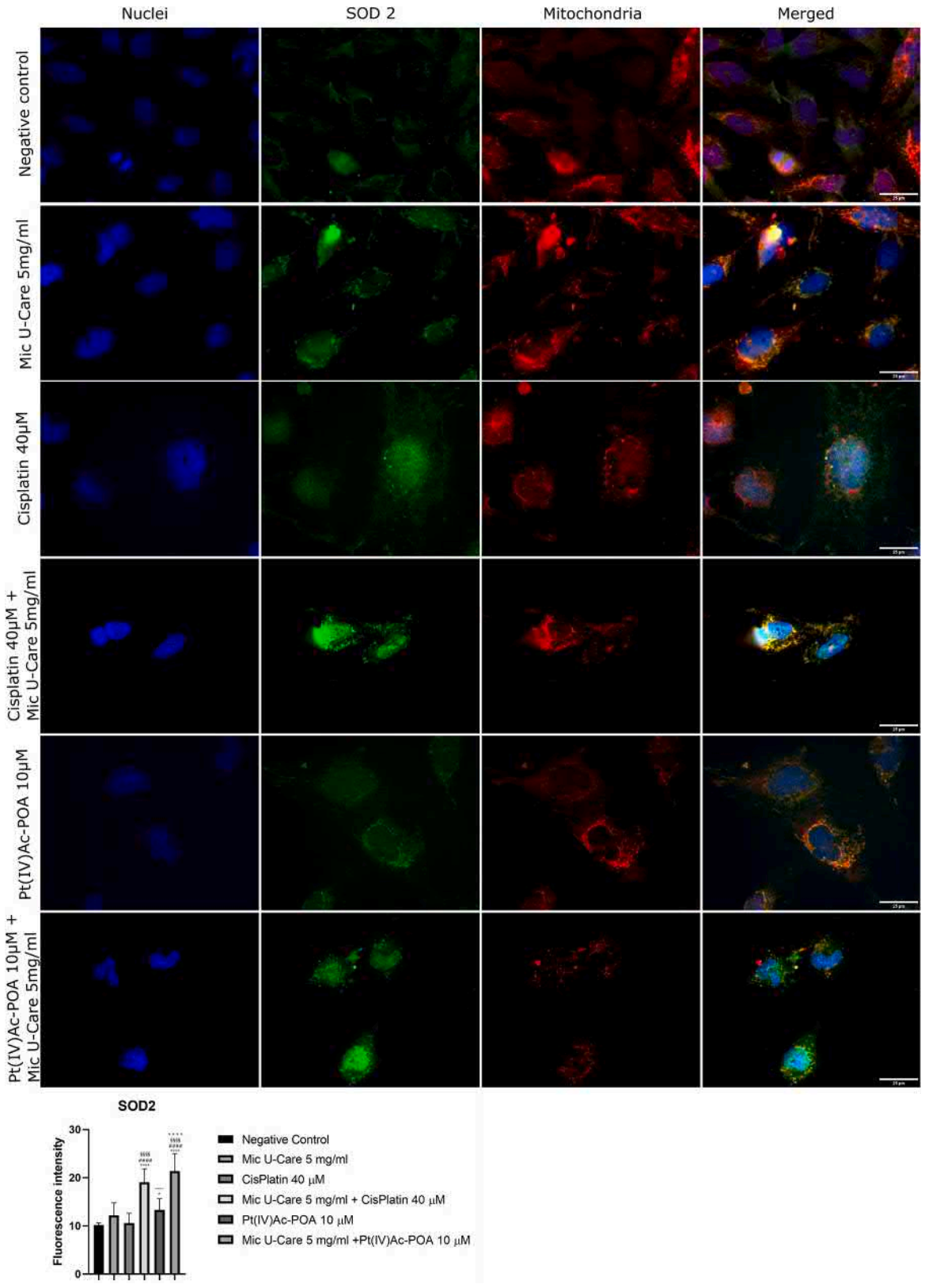

Fig. 4. Double immunolabeling for SOD2 protein (in green) and mitochondria (in red) in the controls, differently treated U251 cells, i.e., after 48 h-CT with Micotherapy U-Care 5 mg/ml, with CDDP 40 µM, with Pt(IV)Ac-POA 10 µM, with Mic U-Care + CDDP, with Mic U-Care + Pt(IV)Ac- POA. DNA was stained with Hoechst 33258 (blue fluorescence). Magnification 60 ×, bar of 25 µm. The histogram below shows the fluorescence intensity value of the immunolabeling. Statistical significance calculated as follows: *control vs. each experimental condition; #Mic U-Care vs. other treatments; §Cisplatin vs. Pt(IV)Ac-POA and each combined treatment; °Cisplatin + Mic U-Care vs. Pt(IV)Ac-POA and Pt(IV)Ac-POA + Mic U-Care; + Pt(IV)Ac-POA vs. Pt(IV)Ac-POA + Mic U-Care. ****$p < 0.0001$. ***$p < 0.001$; **$p < 0.01$; *$p < 0.1$.

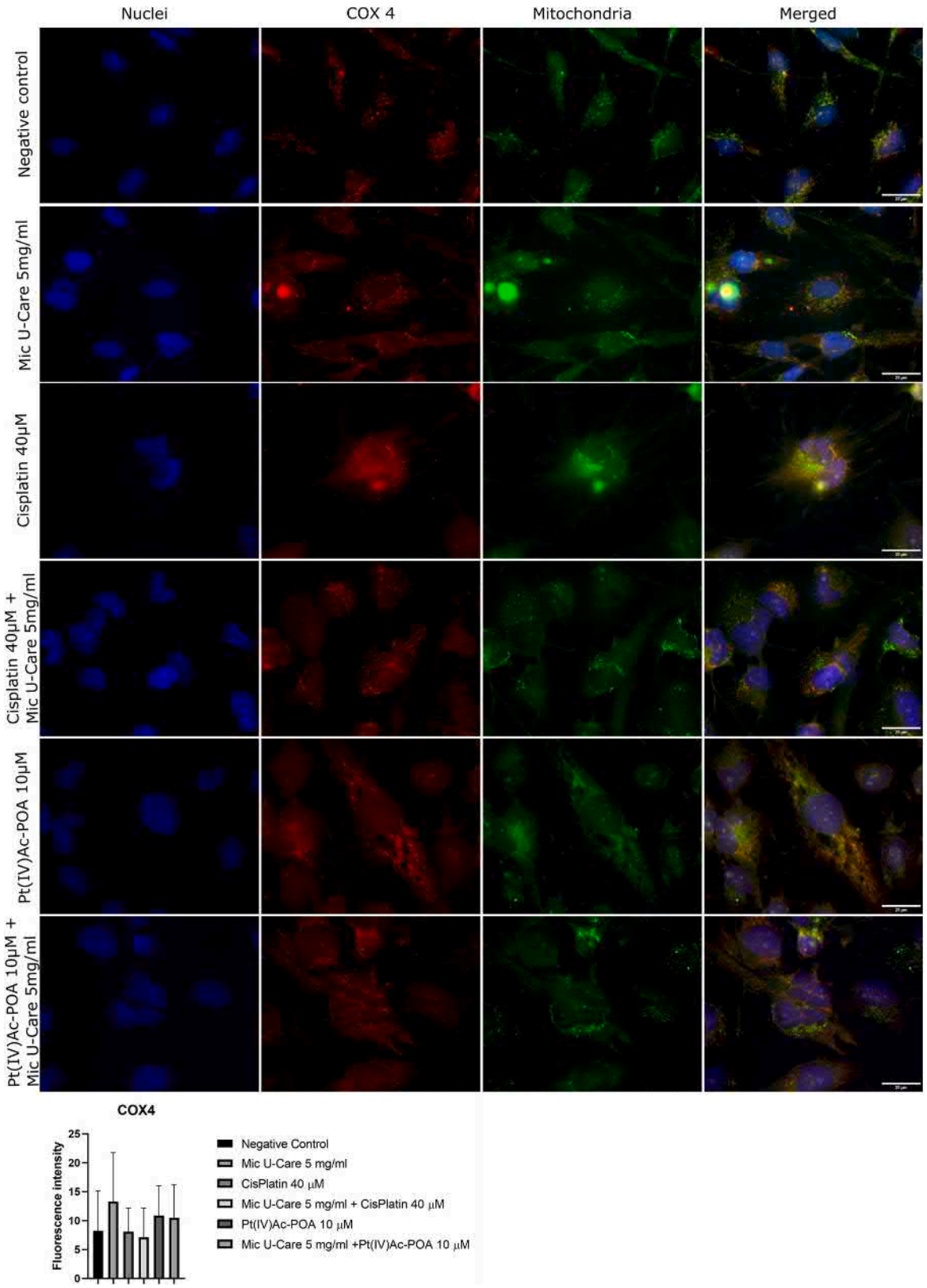

Fig. 5. Double immunolabeling for COX4 (in red) and mitochondria (in green) in the controls, differently treated U251 cells, i.e., after 48 h-CT with Micotherapy U-Care 5 mg/ml, with CDDP 40 μM, with Pt(IV)Ac-POA 10 μM, with Mic U-Care + CDDP, with Mic U-Care + Pt(IV)Ac-POA. DNA was stained with Hoechst 33258 (blue fluorescence). Magnification 60 ×, bar of 25 μm. The histogram below shows the fluorescence intensity value of the immunolabeling. Statistical significance calculated as follows: *control vs. each experimental condition; #Mic U-Care vs. other treatments; §Cisplatin vs. Pt(IV)Ac-POA and each combined treatment; °Cisplatin + Mic U-Care vs. Pt(IV)Ac-POA and Pt(IV)Ac-POA + Mic U-Care; + Pt(IV)Ac-POA vs. Pt(IV)Ac-POA + Mic U-Care. ****$p < 0.0001$. ***$p < 0.001$; **$p < 0.01$; *$p < 0.1$.

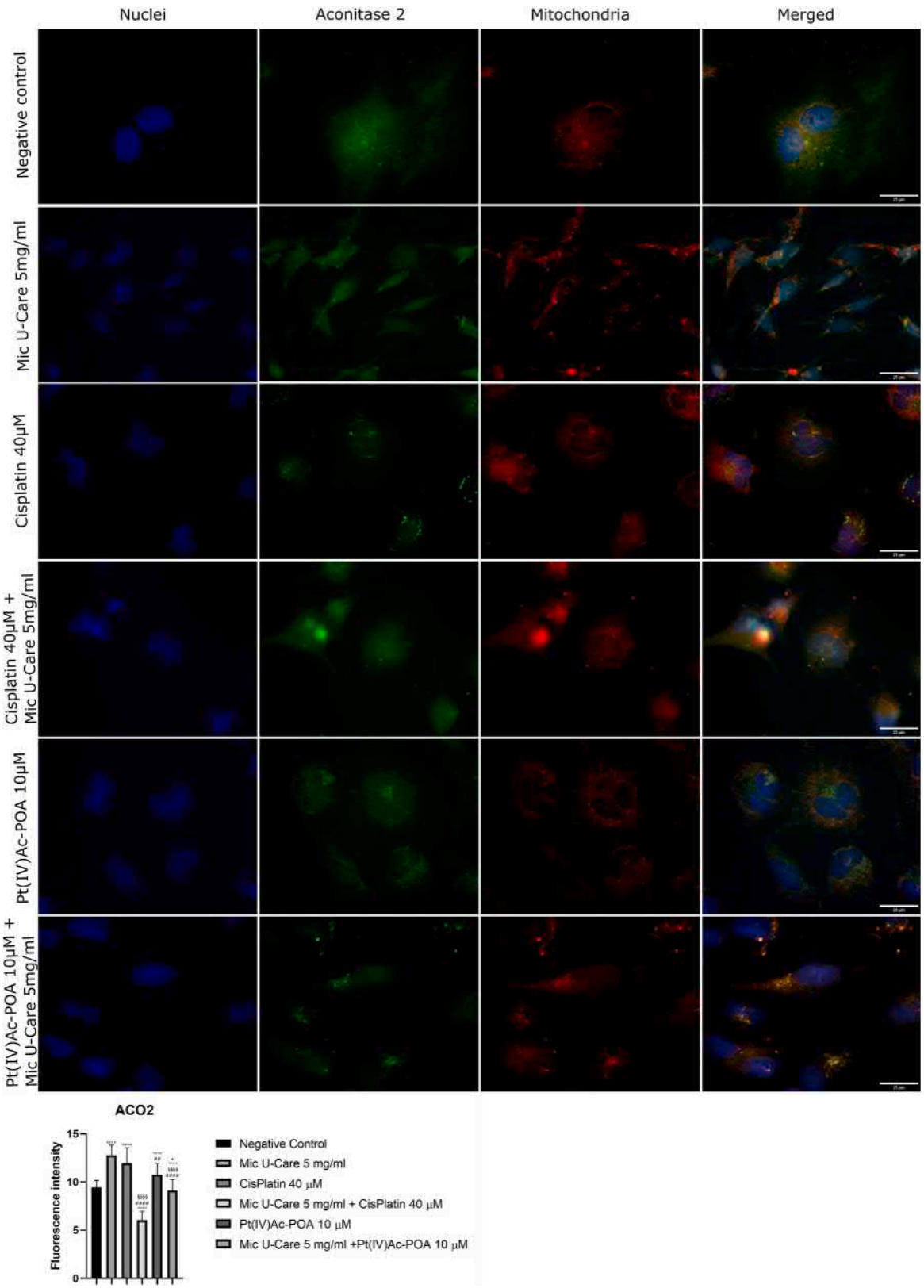

Fig. 6. Double immunolabeling for ACO2 (in green) and mitochondria (in red) in the controls, differently treated U251 cells, i.e., after 48 h-CT with Micotherapy U-Care 5 mg/ml, with CDDP 40 μM, with Pt(IV)Ac-POA 10 μM, with Mic U-Care + CDDP, with Mic U-Care + Pt(IV)Ac-POA. DNA was stained with Hoechst 33258 (blue fluorescence). Magnification 60 ×, bar of 25 μm. The histogram below shows the fluorescence intensity value of the immunolabeling. Statistical significance calculated as follows: *control vs. each experimental condition; #Mic U-Care vs. other treatments; §Cisplatin vs. Pt(IV)Ac-POA and each combined treatment; °Cisplatin + Mic U-Care vs. Pt(IV)Ac-POA and Pt(IV)Ac-POA + Mic U-Care; + Pt(IV)Ac-POA vs. Pt(IV)Ac-POA + Mic U-Care. ****$p < 0.0001$. ***$p < 0.001$; **$p < 0.01$; *$p < 0.1$.

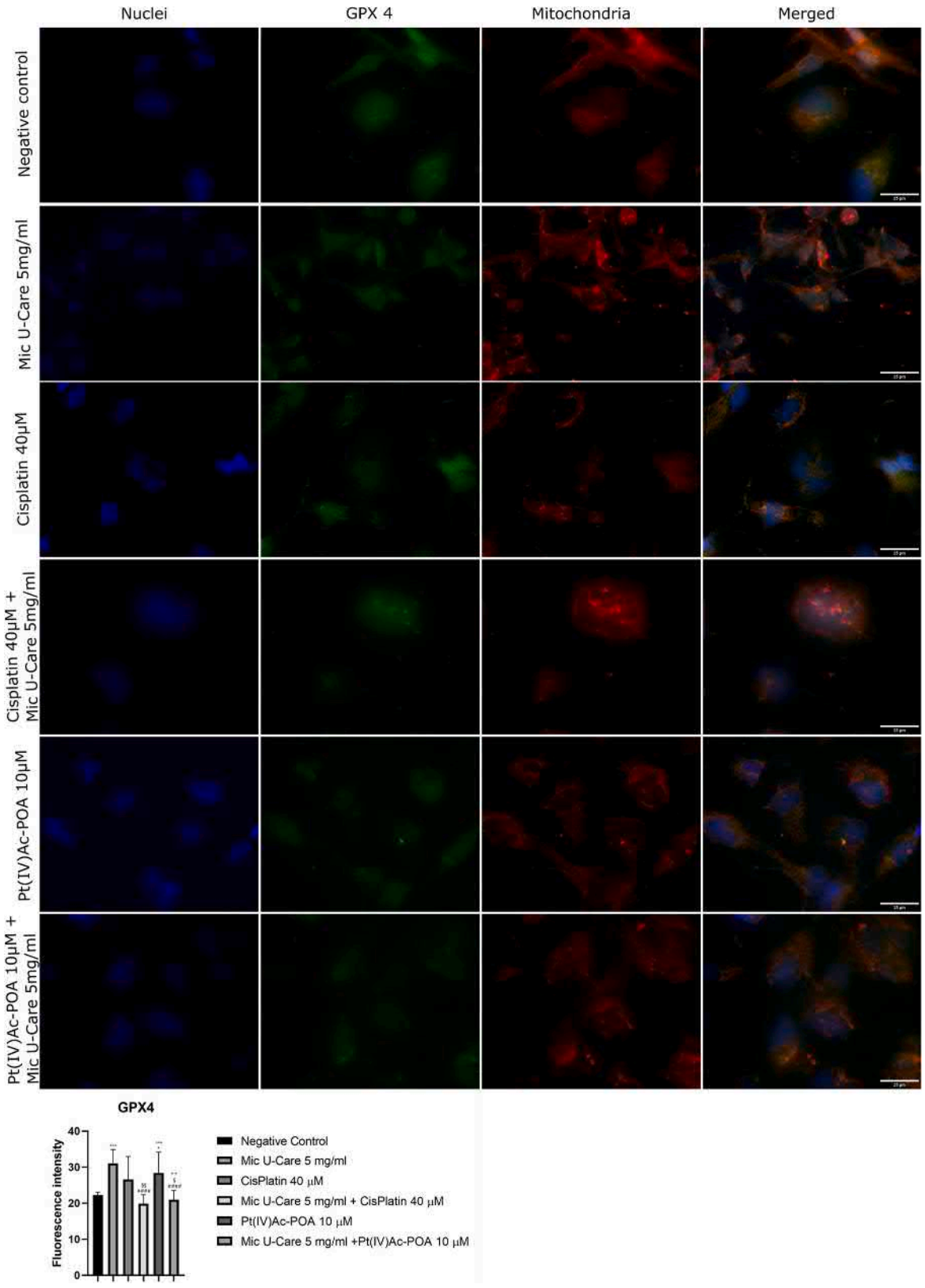

Fig. 7. Double immunolabeling for GPX4 protein (in green) and mitochondria (in red) in the controls, differently treated U251 cells, i.e., after 48 h-CT with Micotherapy U-Care 5 mg/ml, with CDDP 40 µM, with Pt(IV)Ac-POA 10 µM, with Mic U-Care + CDDP, with Mic U-Care + Pt(IV)Ac- POA. DNA was stained with Hoechst 33258 (blue fluorescence). Magnification 60 ×, bar of 25 µm. The histogram below shows the fluorescence intensity value of the immunolabeling. Statistical significance calculated as follows: *control vs. each experimental condition; #Mic U-Care vs. other treatments; §Cisplatin vs. Pt(IV)Ac-POA and each combined treatment; Cisplatin + Mic U-Care vs. Pt(IV)Ac-POA and Pt(IV)Ac-POA + Mic U-Care; + Pt(IV)Ac-POA vs. Pt(IV)Ac-POA + Mic U-Care. ****$p < 0.0001$. ***$p < 0.001$; **$p < 0.01$; *$p < 0.1$.

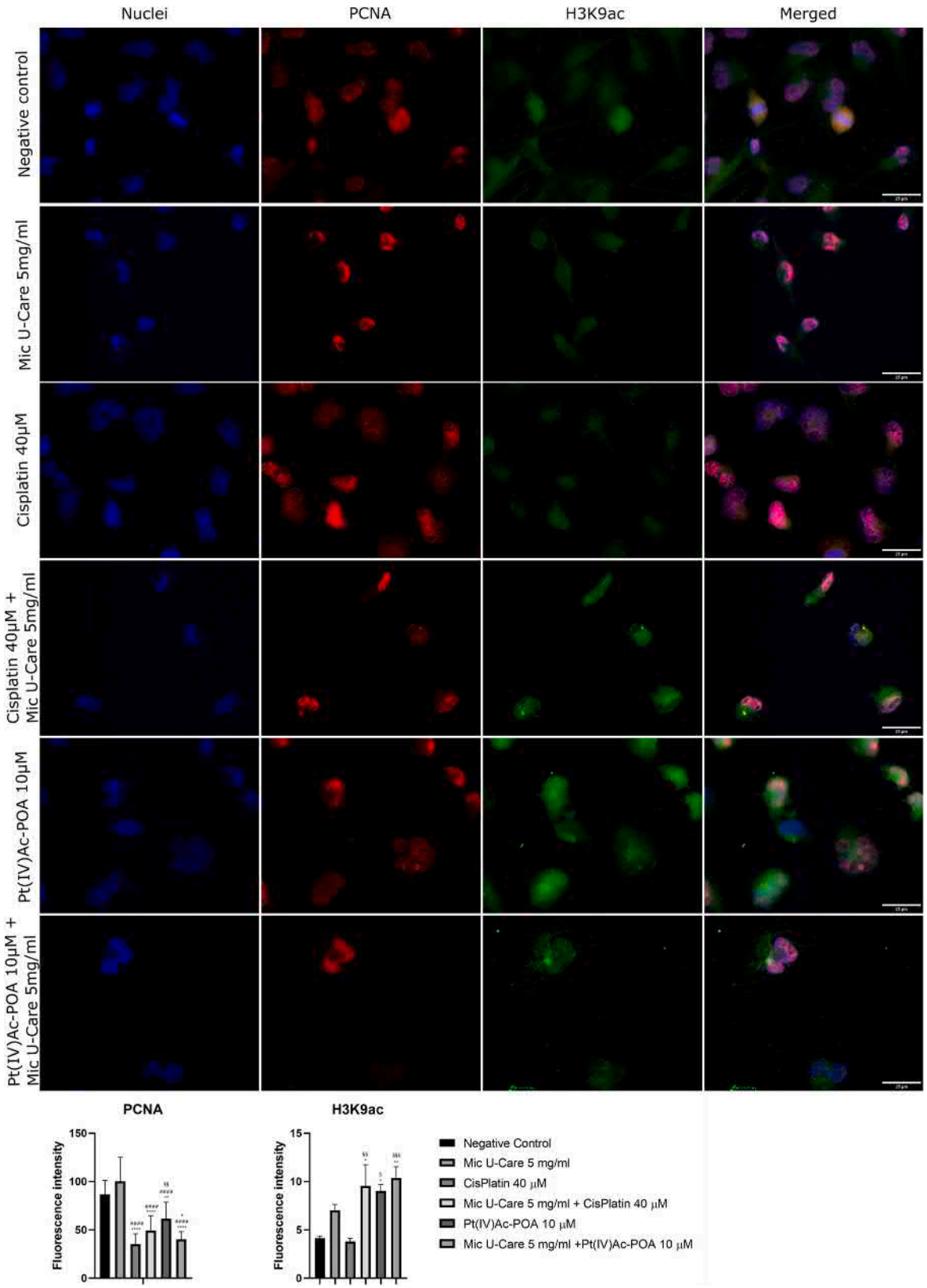

Fig. 8. Double immunolabeling for PCNA protein (in red) and H3K9ac (in green) in the controls, differently treated U251 cells, i.e., after 48 h-CT with Micotherapy U-Care 5 mg/ml, with CDDP 40 µM, with Pt(IV)Ac-POA 10 µM, with Mic U-Care + CDDP, with Mic U-Care + Pt(IV)Ac-POA. DNA was stained with Hoechst 33258 (blue fluorescence). Magnification 60 ×, bar of 25 µm. The histogram below shows the fluorescence intensity value of the immunolabeling. Statistical significance calculated as follows: *control vs. each experimental condition; #Mic U-Care vs. other treatments; §Cisplatin vs. Pt(IV)Ac-POA and each combined treatment; °Cisplatin + Mic U-Care vs. Pt(IV)Ac-POA and Pt(IV)Ac-POA + Mic U-Care; + Pt(IV)Ac-POA vs. Pt(IV)Ac-POA + Mic U-Care. ****$p < 0.0001$. ***$p < 0.001$; **$p < 0.01$; *$p < 0.1$.

with Pt(IV)Ac-POA 10 μM, the results offered also the founding of increasing of histone acetylation in the cells exposed not only to Pt(IV) Ac-POA 10 μM + Mic U-Care 5 mg/ml but to CDDP 40 μM + Mic U-Care 5 mg/ml too. (Cisplatin − 7.91 %, SEM 0.31, Cisplatin + Mic U-Care- + 130.70 %, SEM 2.20 ($\rho = 0.0107$), Pt(IV)Ac-POA + 118.46 %, SEM 0.66 ($\rho = 0.0271$) and Pt(IV)Ac-POA + Mic U-Care + 151.00 %, SEM 1.15 ($\rho = 0.0020$) (all vs. CTR)) (Table 2).

In Fig. 9 was reported the immunofluorescence analysis on CDC42. This small GTPase in active state causes the formation of thin, actin-projections called filopodia. In our samples, it localized on the plasmatic membrane in control condition, after the exposure to Mic U-Care 5 mg/ml and to CDDP 40 μM alone, while in treatment with Pt(IV)Ac-POA 10 μM and combined therapies Pt(IV)Ac-POA 10 μM + Micotherapy U-Care 5 mg/ml the signal was concentrated in the perinuclear area. If in the control samples, in those treated with the micotherapy alone and in those exposed to Cisplatin 40 μM were still recognizable elongated structures, the pseudopods, these have not been found in the other conditions. Promising differences weren't verifiable in the fluorescence intensity among the sample subjected to the different treatment, a slight increasing of CDC42 signal was observable in the cells treated with Cisplatin, while a minor decrease appeared in the samples subjected to Pt(IV)Ac-POA and combined treatments. (Cisplatin + 23.29 %, SEM 1.17, Cisplatin + Mic U-Care − 13.16 %, SEM 0.40, Pt(IV)Ac-POA − 9.84 %, SEM 0.57 and Pt(IV)Ac-POA + Mic U-Care − 17.40 %, SEM 0.46 (all vs. CTR)) (Table 2).

4. Discussion

In the last decade, there have been many articles that have discussed the possibility of the use of antioxidants to assist chemotherapy drugs in the treatment of human cancers. Cancer cells show greater oxidative stress than healthy cells and exploit the upregulated antioxidant system to circumvent the ROS-mediated damage. Recently, the effect of supplementation with antioxidants has been shown to induce a lowering of the toxicity of chemotherapy drugs, inducing greater therapeutic efficiency and an increase in survival times in patients. Roda and collaborators have shown that medicinal mushrooms not only have a range of health benefits [23] but that, due to the presence of bioactive metabolites, they can be used as anticancer agents or in supportive treatment of chemotherapy. In fact, in 4T1 cell line, a triple negative mouse BC model, Micotherapy U-Care, led to a significant reduction in lung metastases with a consequent decrease in oxidative stress and inflammation [21]. The data presented in this work confirm the potential of this supplement. Indeed, the results with the cytofluorimetric analysis show that used at a concentration of 5 mg/ml Micotherapy U-Care determines a decreasing of cells in G1 phase and an increasing of those in G2/M phase, suggesting a cell cycle block in the least. Additionally, the presence of a sub-G1 peak demonstrates the activation of cell death, in the applied condition. Moreover, the analysis relating to PCNA, i.e. Proliferating Cell Nuclear Antigen, a processivity factor for DNA-polymerase-δ, revealed a decrease in proliferative activity in the samples subjected to combined therapy, and in particular following treatment with Micotherapy U-Care and the fourth generation platinum-based derivative. The foundings hint that the use of this supplement could be advantageous for synchronizing cells in a single phase of the cell cycle and afterward subjecting them to targeted chemotherapy treatment.

Promising morphological changes emerge from immunofluorescence and microscopy analysis. After the exposition to the micotherapy, the cell structure is elongated and the nucleus appears more flattened, moreover, cells don't show the typical astrocytic-like structure. In samples treated with chemotherapy there is the collapsing of the cytoskeleton structure that appears also after the combined therapies with a decrease of the cell volume. Only in cells treated with the Mic U-Care alone and in those exposed to Cisplatin pseudopods-like protrusions are still recognizable, suggesting, instead, that Pt(IV)Ac-POA and combined therapy may offer support in the stemming of tumor cell migration. To support this thesis the reduction of the expression of CDC42, small GTPase responsible for the formation of filopodia, in the samples treated with the combination of micotherapy and chemotherapy compared to the corresponding chemotherapy alone.

Therefore, if after the exposition to the chemotherapy alone elongated mitochondria are visible in U251 cells, after combined therapy, this typical feature of drug resistance mechanism is lacking. Conversely, in samples subjected to Micotherapy U-Care and chemotherapy together an accumulation of mitochondria in the nuclear periphery is visible, probably as the result of a collapsed cytosolic organization.

Shrinkage of mitochondria and reduction of mitochondrial crests can be feature of an inadequate response to oxidative stress conditions, at the same time, mitochondrial dynamics is crucial for cellular survival [14]. Mitochondrial stress triggers an inflammatory phenotype, with the activation of the OPA1 protein whose role is essential in the maintenance of normal mitochondrial crests and for protecting cells from apoptosis by preventing the release of cytochrome c [9]. Our studies support an increasing of this large GTPase in samples treated with chemotherapeutic agents alone, while the synergistic pharmacological action of the tested compounds seem to maintain the basal expression of OPA1, opening for a reduction of the capability of the tumoral cells to adapt to the anticancer therapy due to the use of the micotherapy. Further studies will be conducted to evaluate the presence of a relation between the expression of OPA1 and the kind of cell death that could interests our cell type after the treatment with Micotherapy U-Care, platinum-based chemotherapy and the combination of the two.

An enhanced defect in mitochondrial function after samples exposition to combined therapy is supported also by the decreased expression of COX4 cells treated with Micotherapy U-Care + chemotherapy, compared to respective chemotherapies used alone. COX4 levels alteration could potentially lead to the accumulation of ROS and oxidative stress in mitochondria, it has to be evaluated if this event induces the activation of the mitophagic pathway in our samples. However, it is known that COX4 under-regulation has effects on mitochondrial respiration and ATP production, resulting in induction of cell death pathways [19].

Successively, the study of redox condition reveals an increasing of the expression of SOD1 and SOD2 in samples treated with combined therapy and with micotherapy alone, these results can be significant of reduction of oxidative stress and therefore of a reduced tumorigenesis favored by the usage of Mic U-Care, since ROS can promote metastases proliferation due to DNA mutations. Recently, substances of vegetable origin have been added to chemotherapeutics, in particular mushrooms, used because they are considered as adjuvants in the response to drug therapies, as showed by Roda et al. [21].

It might be interesting to evaluate the interaction between SODs and proteins belonging to the sirtuins family (SIRT). SIRT1 is a NAD^+-dependent histone lysine deacetylase that, among other things, regulates the acetylation of the K70 residue in SOD1 which could consequently inactivate the formation of the homodimer and therefore the correct functionality of the molecule. Sirtuin 1 is overexpressed in many types of solid tumors and hematopoietic neoplasms and is linked to the development of drug resistance capability [26].

Another demonstration of mitochondrial disfunction favored by the administration of Micotherapy U-Care can be found in the reduction of ACO2 expression in combined therapy compared to chemotherapy alone. In particular, a decreasing of ACO2 seems to be linked to the release of Fe^{2+} and H_2O_2 ion, and, therefore, to the activation of autophagy and/or mitophagy as well as oxidative stress and ferroptosis, harmful to cancer cells.

Ferroptosis is a form of regulated cell death, caused by excessive iron-dependent lipid peroxidation, it can be initiated by iron-induced ROS production through the Fenton reaction, or by the activation of iron-containing enzymes [15]. GPX4, glutathione peroxidase 4, acting as a phospholipid hydroperoxidase is involved in the antiferroptotic

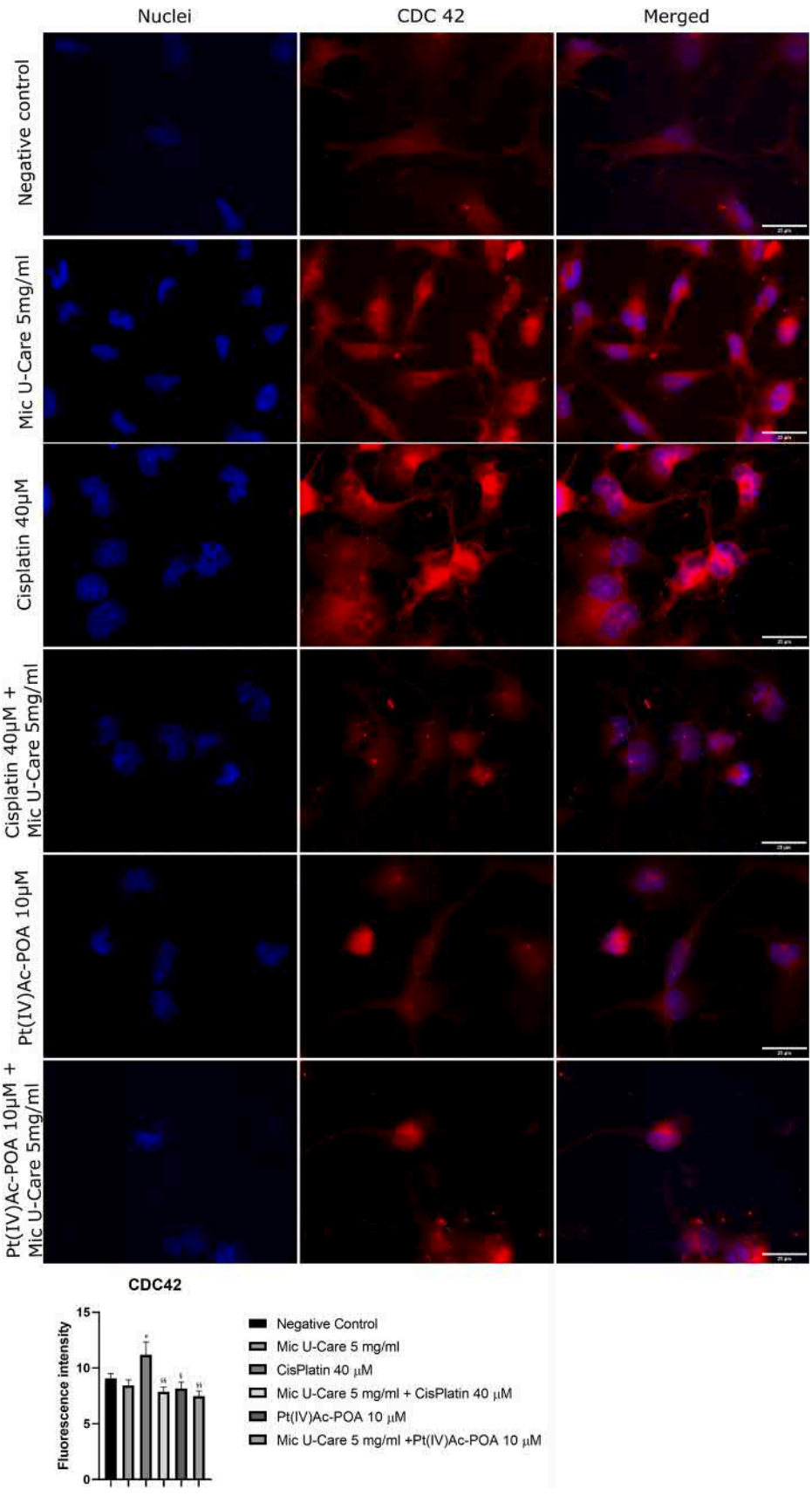

Fig. 9. Immunolabeling for CDC42 (in red) in the controls, differently treated U251 cells, i.e., after 48 h-CT with Micotherapy U-Care 5 mg/ml, with CDDP 40 µM, with Pt(IV)Ac-POA 10 µM, with Mic U-Care + CDDP, with Mic U-Care + Pt(IV)Ac-POA. DNA was stained with Hoechst 33258 (blue fluorescence). Magnification 60 ×, bar of 25 µm. The histogram below shows the fluorescence intensity value of the immunolabeling. Statistical significance calculated as follows: *control vs. each experimental condition; #Mic U-Care vs. other treatments; §Cisplatin vs. Pt(IV)Ac-POA and each combined treatment; °Cisplatin + Mic U-Care vs. Pt (IV)Ac-POA and Pt(IV)Ac-POA + Mic U-Care; + Pt (IV)Ac-POA vs. Pt(IV)Ac-POA + Mic U-Care. ****$p < 0.0001$. ***$p < 0.001$; **$p < 0.01$; *$p < 0.1$.

activity of GSH. GPX4 expression decreased in samples receiving combination therapy in comparison with the counterpart chemotherapy. This may be indicative of increased sensitivity to ferroptosis following combined therapy. Further ferroptosis markers (e.g.: BAP1 and NRF2) will be studied to investigate the activation-mechanisms of this cell death pathway.

5. Conclusions

The results of the present study suggest that micotherapy effect can be synergic to the one of chemotherapy, moreover, the use of micotherapy could favor the control of oxidative stress states with the reduction of the induction of inflammatory conditions in the tumor microenvironment while not negatively affecting the control of proliferation and migration processes and the activation of programmed cell death. Thus, fungi can act as an enhancers of host defense mechanisms and decrease adverse effects events in cancer patients undergoing conventional therapies.

New protocols for clinical studies are needed to elucidate the possible active mechanisms and clinical benefits of these fungi on various types of cancer.

Credit authorship contribution statement

All authors contributed to the study, conception and design. Experiments and data analyses were performed by L.G, E.R, C.F, F.G, E.G. M.R and P.R. provided critical materials. M.G.B: supervised the study. The first draft of the manuscript was written by L.G and all authors commented on previous versions of the manuscript. All authors read and approved the final manuscript.

Ethics approval

Not applicable.

Funding

This research was supported by the University of Pavia: Fondi Ricerca Giovani (FRG 2020). We are indebted to the Inter-University Consortium for Research on the Chemistry of Metals in Biological Systems (CIRCMSB, Bari) for stimulating discussions during the group meetings and short-term missions. This research was supported by Italian Ministry of Education, University and Research (MIUR): Department of Excellence Program (2018–2022) - Dept. of Biology and Biotechnology "L. Spallanzani", University of Pavia.

Conflict of interest

The authors declare no competing interests.

Data Availability

Data sharing not applicable to this article as no datasets were generated or analyzed during the current study.

Acknowledgments

We thank Dr. Giuliano Mazzini (IGM-CNR, Pavia) for his excellent assistance in the analysis in flow cytometry.

Consent to participate

Not applicable.

Authors' Information

All authors contributed to the study and they all read and approved the final manuscript. Maria Grazia Bottone is the corresponding author.

Consent for publication

All authors have given consent to publication of the manuscript.

References

[1] M. Bourens, F. Fontanesi, I.C. Soto, J. Liu, A. Barrientos, Redox and reactive oxygen species regulation of mitochondrial cytochrome C oxidase biogenesis, Antioxid. Redox Signal. 19 (16) (2013) 1940–1952, https://doi.org/10.1089/ars.2012.4847.
[2] C.H. Chien, W.T. Hsueh, J.Y. Chuang, K.Y. Chang, Dissecting the mechanism of temozolomide resistance and its association with the regulatory roles of intracellular reactive oxygen species in glioblastoma, J. Biomed. Sci. 28 (1) (2021) 1–10, https://doi.org/10.1186/s12929-021-00717-7.
[3] F. Ciccarone, L. Di Leo, G. Lazzarino, et al., Aconitase 2 inhibits the proliferation of MCF-7 cells promoting mitochondrial oxidative metabolism and ROS/FoxO1-mediated autophagic response, Br. J. Cancer 122 (2020) 182–193, https://doi.org/10.1038/s41416-019-0641-0.
[4] B. Ferrari, E. Roda, E.C. Priori, F. De Luca, A. Facoetti, M. Ravera, F. Brandalise, C. A. Locatelli, P. Rossi, M.G. Bottone, A new platinum-based prodrug candidate for chemotherapy and its synergistic effect with hadrontherapy: novel strategy to treat glioblastoma, Front. Neurosci. 15 (March) (2021) 1–28, https://doi.org/10.3389/fnins.2021.589906.
[5] B. Ferrari, F. Urselli, M. Gilodi, S. Camuso, E.C. Priori, B. Rangone, M. Ravera, P. Veneroni, I. Zanellato, E. Roda, D. Osella, M.G. Bottone, New platinum-based prodrug Pt(IV)Ac-POA: antitumour effects in rat C6 glioblastoma cells, Neurotox. Res. 37 (1) (2020) 183–197, https://doi.org/10.1007/s12640-019-00076-0.
[6] E.H. Fyllingen, L.E. Bø, I. Reinertsen, A.S. Jakola, L.M. Sagberg, E.M. Berntsen, Ø. Salvesen, O. Solheim, Survival of glioblastoma in relation to tumor location: a statistical tumor atlas of a population-based cohort, Acta Neurochir. 163 (7) (2021) 1895–1905, https://doi.org/10.1007/s00701-021-04802-6.
[7] S. Galadari, A. Rahman, S. Pallichankandy, F. Thayyullathil, Reactive oxygen species and cancer paradox: to promote or to suppress, Free Radic. Biol. Med. 104 (January) (2017) 144–164, https://doi.org/10.1016/j.freeradbiomed.2017.01.004.
[8] L. Galluzzi, L. Senovilla, I. Vitale, J. Michels, I. Martins, O. Kepp, M. Castedo, G. Kroemer, Molecular mechanisms of cisplatin resistance, Oncogene 31 (15) (2012) 1869–1883, https://doi.org/10.1038/onc.2011.384.
[9] R. Gilkerson, P. De La Torre, S. St. Vallier, Mitochondrial OMA1 and OPA1 as gatekeepers of organellar structure/function and cellular stress response, Front. Cell Dev. Biol. 9 (March) (2021) 1–7, https://doi.org/10.3389/fcell.2021.626117.
[10] M. Grimaldi, V.D. Bo, B. Ferrari, E. Roda, F. De Luca, P. Veneroni, et al., Long-term effects after treatment with platinum compounds, cisplatin and [Pt(O,O′-acac)(γ-acac)(DMS)]: autophagy activation in rat B50 neuroblastoma cells, Toxicol. Appl. Pharm. 364 (2019) 1–11, https://doi.org/10.1016/j.taap.2018.12.005.
[11] H. Huang, S. Zhang, Y. Li, Z. Liu, L. Mi, Y. Cai, X. Wang, L. Chen, H. Ran, D. Xiao, F. Li, J. Wu, T. Li, Q. Han, L. Chen, X. Pan, H. Li, T. Li, K. He, J. Man, Suppression of mitochondrial ROS by prohibitin drives glioblastoma progression and therapeutic resistance, Nat. Commun. 12 (1) (2021) 1–16, https://doi.org/10.1038/s41467-021-24108-6.
[12] M. Jermini, J. Dubois, P.Y. Rodondi, K. Zaman, T. Buclin, C. Csajka, A. Orcurto, L. E. Rothuizen, Complementary medicine use during cancer treatment and potential herb-drug interactions from a cross-sectional study in an academic centre, Sci. Rep. 9 (1) (2019) 1–11, https://doi.org/10.1038/s41598-019-41532-3.
[13] X. Jiang, B.R. Stockwell, M. Conrad, Ferroptosis: mechanisms, biology and role in disease, Nat. Rev. Mol. Cell Biol. 22 (4) (2021) 266–282, https://doi.org/10.1038/s41580-020-00324-8.
[14] Y.G. Lee, D.H. Park, Y.C. Chae, Role of mitochondrial stress response in cancer progression, Cells 11 (5) (2022) 1–21, https://doi.org/10.3390/cells11050771.
[15] J. Liu, R. Kang, D. Tang, Signaling pathways and defense mechanisms of ferroptosis, FEBS J. (2021) 1–13, https://doi.org/10.1111/febs.16059.
[16] Y. Liu, Q. Li, L. Zhou, N. Xie, E.C. Nice, H. Zhang, C. Huang, Y. Lei, Cancer drug resistance: redox resetting renders a way, Oncotarget 7 (27) (2016) 42740–42761, https://doi.org/10.18632/oncotarget.8600.
[17] O.V. Lushchak, M. Piroddi, F. Galli, V.I. Lushchak, Aconitase post-translational modification as a key in linkage between Krebs cycle, iron homeostasis, redox signaling, and metabolism of reactive oxygen species, Redox Rep.: Commun. Free Radic. Res. 19 (1) (2014) 8–15, https://doi.org/10.1179/1351000213Y.0000000073.
[18] C. Olivier, L. Oliver, L. Lalier, F.M. Vallette, Drug resistance in glioblastoma: the two faces of oxidative stress, Front. Mol. Biosci. 7 (January) (2021) 1–16, https://doi.org/10.3389/fmolb.2020.620677.
[19] S.M. Pauff, S.C. Miller, Regulation of mitochondrial respiration and apoptosis through cell signaling: cytochrome c oxidase and cytochrome c in ischemia/reperfusion injury and inflammation, Biochim Biophys. Acta 1817 (4) (2012) 598–609, https://doi.org/10.1016/j.bbabio.2011.07.001.
[20] B. Rangone, B. Ferrari, V. Astesana, I. Masiello, P. Veneroni, I. Zanellato, D. Osella, M.G. Bottone, A new platinum-based prodrug candidate: its anticancer effects in

B50 neuroblastoma rat cells, Life Sci. 210 (2018) 166–176, https://doi.org/10.1016/j.lfs.2018.08.048.
[21] E. Roda, F. De Luca, C. Di Iorio, D. Ratto, S. Siciliani, B. Ferrari, F. Cobelli, G. Borsci, E.C. Priori, S. Chinosi, A. Ronchi, R. Franco, R. Di Francia, M. Berretta, C. A. Locatelli, A. Gregori, E. Savino, M.G. Bottone, P. Rossi, Novel medicinal mushroom blend as a promising supplement in integrative oncology: a multi-tiered study using 4t1 triple-negative mouse breast cancer model, Int. J. Mol. Sci. 21 (10) (2020) 1–28, https://doi.org/10.3390/ijms21103479.
[22] G. Santin, V.M. Piccolini, S. Barni, P. Veneroni, V. Giansanti, V. Dal Bo, G. Bernocchi, M.G. Bottone, Mitochondrial fusion: a mechanism of cisplatin-induced resistance in neuroblastoma cells, Neurotoxicology 34 (2013) (2013) *51–60*, https://doi.org/10.1016/j.neuro.2012.10.011.
[23] E. Roda, D. Ratto, F. De Luca, A. Desiderio, M. Ramieri, L. Goppa, E. Savino, M. G. Bottone, C.A. Locatelli, P. Rossi, Searching for a longevity food, we bump into hericium erinaceus primordium rich in ergothioneine: the "longevity vitamin" improves locomotor performances during aging, Nutrients 14 (6) (2022), https://doi.org/10.3390/nu14061177.
[24] P. Tagde, P. Tagde, S. Tagde, T. Bhattacharya, V. Garg, R. Akter, M.H. Rahman, A. Najda, G.M. Albadrani, A.A. Sayed, M.F. Akhtar, A. Saleem, A.E. Altyar, D. Kaushik, M.M. Abdel-Daim, Natural bioactive molecules: an alternative approach to the treatment and control of glioblastoma multiforme, Biomed. Pharmacother. 141 (April) (2021), 111928, https://doi.org/10.1016/j.biopha.2021.111928.
[25] D. Trachootham, J. Alexandre, P. Huang, Targeting cancer cells by ROS-mediated mechanisms: a radical therapeutic approach, Nat. Rev. Drug Discov. 8 (7) (2009) 579–591, https://doi.org/10.1038/nrd2803.
[26] Z. Wang, W.Y. Chen, Emerging roles of SIRT1 in cancer drug resistance, Genes Cancer 4 (3–4) (2013) 82–90, https://doi.org/10.1177/1947601912473826.
[27] S.Y. Yin, W.C. Wei, F.Y. Jian, N.S. Yang, Therapeutic applications of herbal medicines for cancer patients, Evid.-Based Complement. Altern. Med., 2013, 2013 (Table 1). ⟨https://doi.org/10.1155/2013/302426⟩.
[28] J.F. Ying, Z.B. Lu, L.Q. Fu, Y. Tong, Z. Wang, W.F. Li, X.Z. Mou, The role of iron homeostasis and iron-mediated ROS in cancer, Am. J. Cancer Res. 11 (5) (2021) 1895–1912.
[29] S. Zhang, W. Xin, G.J. Anderson, et al., Double-edge sword roles of iron in driving energy production versus instigating ferroptosis, Cell Death Dis. 13 (2022) 40, https://doi.org/10.1038/s41419-021-04490-1.